Duct-ventilated embankment

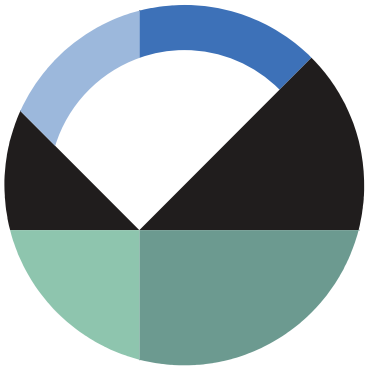

GEO-SLOPE International Ltd. | www.geo-slope.com

1200, 700 - 6th Ave SW, Calgary, AB, Canada T2P 0T8
Main: +1 403 269 2002 | Fax: +1 888 463 2239

Introduction

The construction of roadway and railway embankments in cold regions can influence the overall thermal response of underlying permafrost. This change in the thermal regime can lead to thermal degradation and an unstable foundation. The use of duct ventilation along the embankment has been found to prevent, or at least slow down, the degradation process when compared to conventional embankments (Zarling et al., 1984, Li et al., 2006, and Yu et al, 2008). In this example, the thermal response of a duct-ventilated embankment, with temperature-controlled shutters, is compared to that of a conventional embankment using TEMP3D.

Numerical Simulation

The roadway embankment in this example is 2.5 m high and 18 m wide, with 2:1 side-slopes. The circular ducts are placed perpendicular to the road alignment, at a spacing of 2 m on the duct center, and 0.5 m above the original ground surface. In this particular analysis, the 0.2 m diameter ducts are provided with temperature-controlled shutters that are designed to close as the air temperature rises above 0°C. Using symmetry, the domain is simplified to half of the embankment width over the mid-pipe distance (refer to Figure 1). For comparison purposes, a second three-dimensional (3D) geometry was created without ducts to simulate a conventional embankment. In both cases, the embankment is underlain by a 9 m deep, 17 m wide, silty foundation.

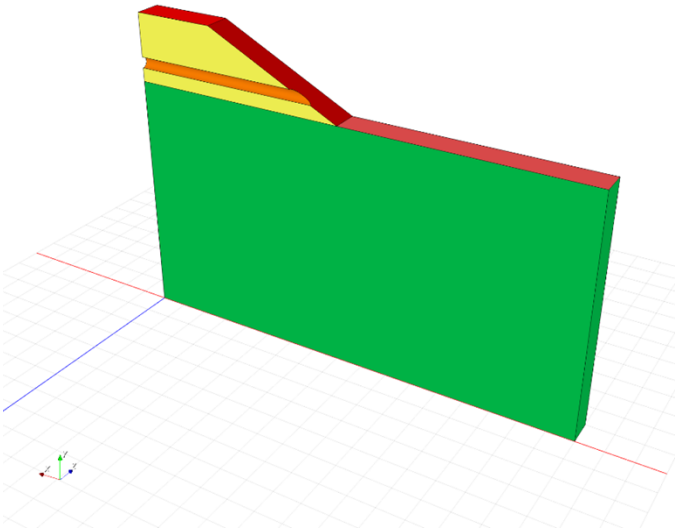

Figure 1. Configuration of 3D geometry.

The embankment and foundation materials are both defined using the Full Thermal Material Model. The embankment material consists of a relatively dry sand/gravel mixture with a volumetric water content of 0.1 m^3/m^3. The frozen and unfrozen volumetric heat capacity of the mixture is equal to 1620 $kJ/m^3/°C$ and 1990 $kJ/m^3/°C$, respectively. The thermal conductivity function is estimated using the sample sand material with a frozen and unfrozen thermal conductivity of 2.15 J/sec/m/°C and 1.99 J/sec/m/°C, respectively. The foundation consists of an ice-rich silt with a volumetric water content of 0.649 m^3/m^3. The frozen and unfrozen volumetric heat capacity of the silt is equal to 2380 $kJ/m^3/°C$ and 3740 $kJ/m^3/°C$, respectively. The thermal conductivity function, on the other hand, is estimated using the sample silt material, with a frozen and unfrozen thermal conductivity of 2.32 J/sec/m/°C and 1.49 J/sec/m/°C, respectively. Figure 2 shows the normalized unfrozen volumetric water content function of each of these materials.

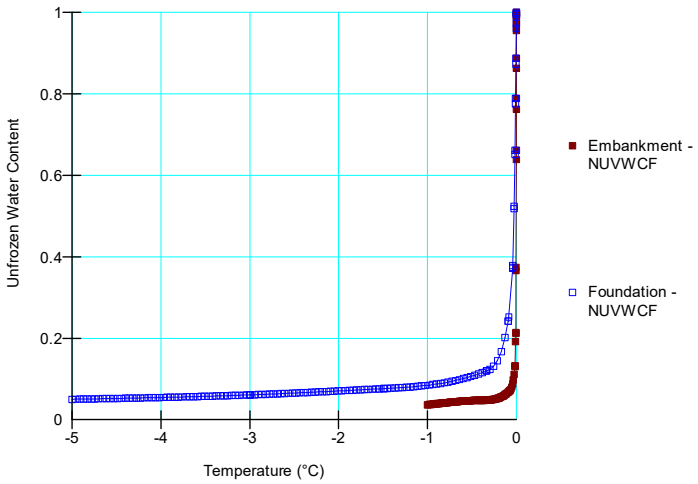

Figure 2. Normalized unfrozen volumetric water content functions of the embankment and foundation materials.

The air temperature, shown in Figure 3, is representative of conditions in Fairbanks, Alaska. The temperatures on the roadway, embankment side-slope, and foundation surfaces are computed using the n-factors provided in Table 1. The initial temperature of the embankment and foundation materials are based on average annual surface temperatures, and are set to 1.9551 °C and -1.8948 °C, respectively.

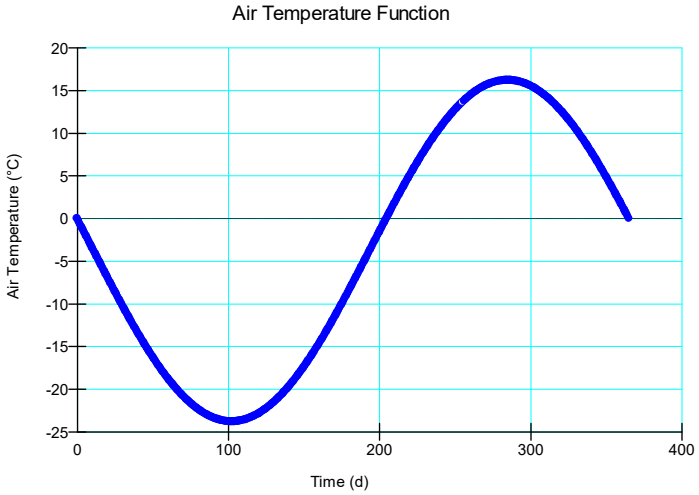

Figure 3. Air temperature function (Goering and Kumar, 1996).

Table 2. Thawing and freezing n-factors used in the thermal boundary conditions for each surface type (from Goering and Kumar, 1996).

Surface type	Freezing n-factor	Thawing n-factor
Embankment top (roadway surface)	0.9	1.9
Embankment side-slope	0.6	1.7
Foundation	0.5	0.5

A Convective Surface boundary condition is used to simulate the conditions on the inner surface of the ventilation duct. The convective heat transfer coefficient is set equal to 0.01 kJ/s/m²/°C when the shutters are open (and the temperature is below 0°C), and 0 kJ/s/m²/°C when the shutters are closed (and the temperature is above 0°C). The aforementioned convective heat transfer coefficient is consistent with that reported in Zarling et al. (1984). A geothermal heat flux of 6.0 x 10^{-5} kJ/sec/m² is applied to the bottom boundary of the domain.

The domain is predominantly characterized by tetrahedral elements, with a default edge length of 0.5 m. A mesh constraint is applied to the inner surface of the ventilation duct, in the embankment body, and along the embankment/foundation interface to improve results near the 0°C isoline. The resulting mesh consists of 10492 nodes and 60368 elements.

In order to eliminate the effect of the initial conditions, the duration of both analyses is set equal to 3650 days (or 10 years). Convergence is ensured by using 4-hour time steps. Note, the duration of the analyses in the accompanying file has been set to 10 days to reduce file size.

Results and Discussion

Figure 4 shows the temperature at the center of the embankment/foundation interface on August 1st of each simulated year. As expected, the temperatures increase exponentially, and eventually reach constant, annually-reproducible values. At this point, the effect of the initial conditions has been removed, and the different mitigation measures can be evaluated. Note that the time required to reach a constant temperature is larger in the conventional embankment given that it results in greater warming of the underlying permafrost. The duct-ventilated embankment generally leads to colder temperatures, and shorter stabilization times.

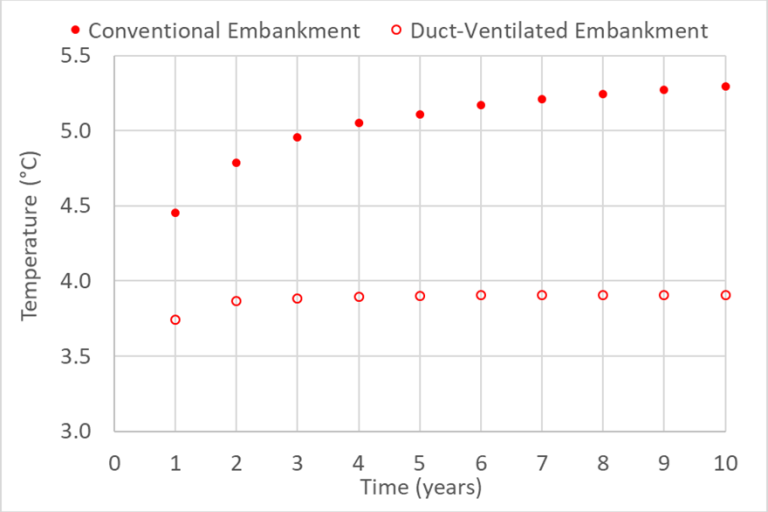

Figure 4. Temperature at the center of the embankment/foundation interface on August 1st of each year.

Figure 5 shows the temperature contour plot on August 1st of the last year of the simulation, when temperatures are warmest. As expected, the duct-ventilated embankment results in a colder permafrost. Figure 6 shows the temperature versus time at different points in the domain during the last year of simulation, and further illustrates the cooling effect of the duct-ventilated embankment. A close look at the results reveals that the temperature at the center of the embankment/foundation interface reaches a minimum of -15.5°C during wintertime, which is much colder than the temperatures observed below the conventional embankment. As a result of the temperature-controlled shutters, the temperatures during summertime never exceed 4.0°C.

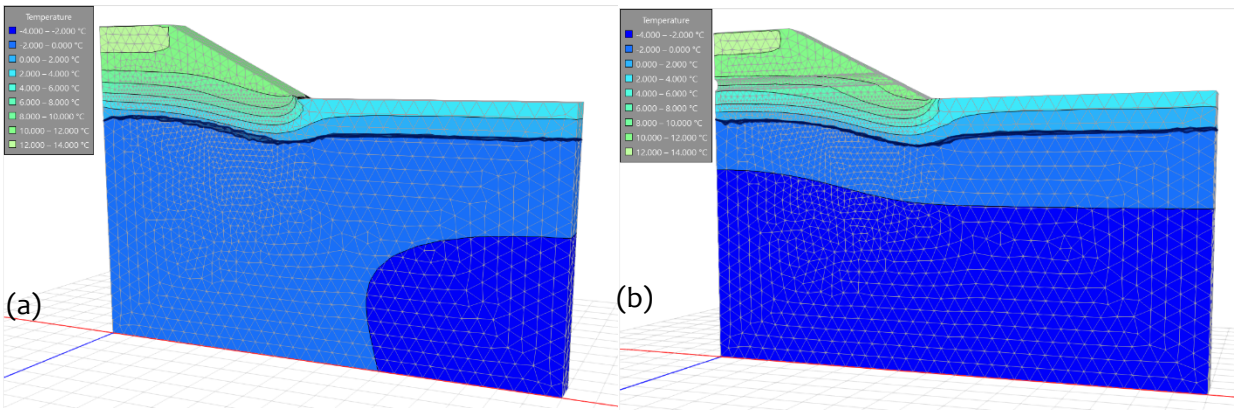

Figure 5. Temperature contour plot and zero isosurface on August 1st of the last year of simulation for the (a) conventional embankment, and (b) duct-ventilated embankment.

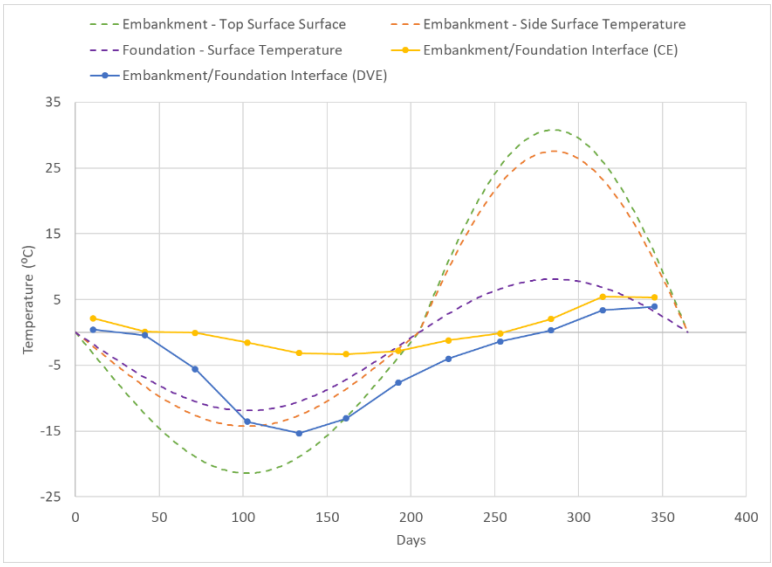

Figure 6. Temperature versus time at different points in the domain during the final year of the simulation.

Figure 7 shows the temperature profile (or trumpet plot) at the centerline during the last year of simulation. The duct-ventilated embankment clearly leads to a larger active region, and much colder permafrost. More specifically, the yearly average temperature of the permafrost is -3.0°C with duct ventilation and -0.75°C without duct ventilation. These findings are in complete agreement with those of other numerical studies on duct-ventilated embankments (Li et al., 2006; Yu et al., 2008).

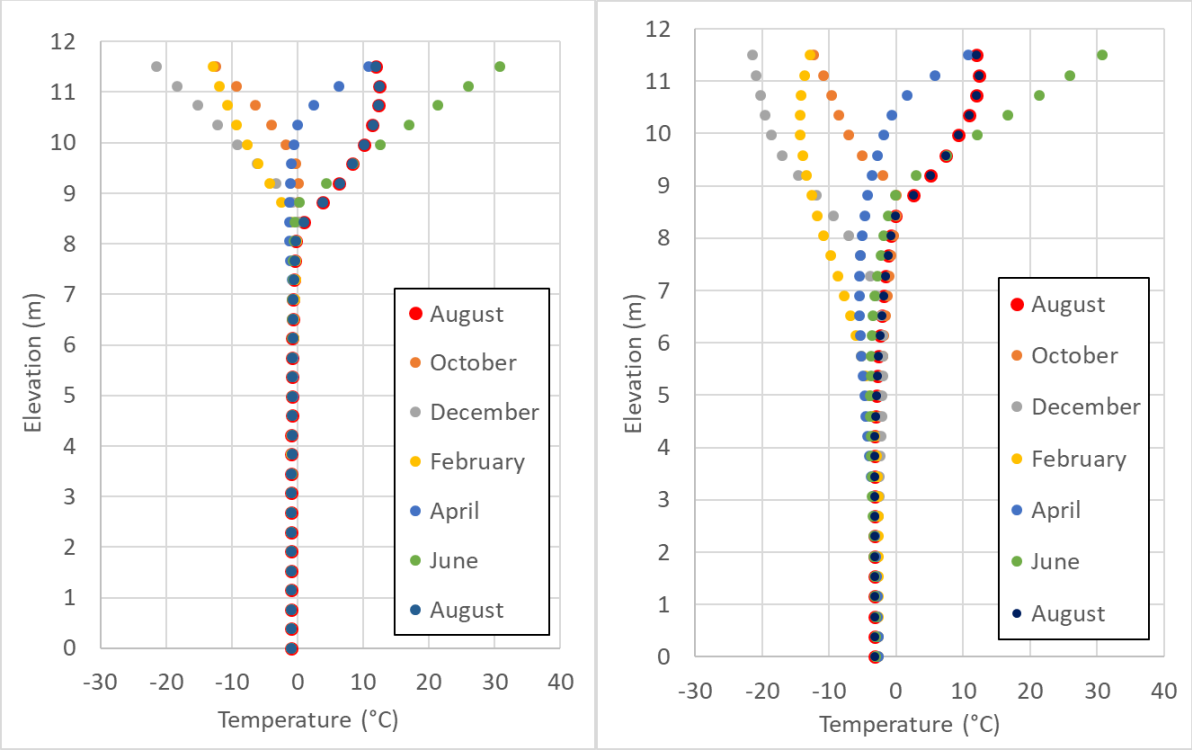

Figure 7. Temperature profiles at the centerline (midpoint between ducts) during the last year of simulation.

Summary and Conclusions

TEMP3D was used to model conductive heat transfer in embankments with and without duct ventilation. The duct-ventilated embankment with temperature-controlled shutters was shown to provide colder permafrost conditions than a conventional embankment. A more efficient response could have been achieved by moving the duct closer to the embankment/foundation interface and/or by decreasing the spacing of the ducts. Although herein placed perpendicular to the roadway alignment, the ventilation ducts could also have been placed longitudinally, near the embankment toe, to reduce differential thawing and embankment rotation.

Reference

Goering, D. J. and Kumar, P. 1996. Winter-time convection in open-graded embankments. Cold Regions Science and Technology 24: 57-74.

Li, G., Li, N., and Quan, X. 2006. The temperature features for different ventilated-duct embankments with adjustable shutters in the Qinghai-Tibet railway. Cold Regions Science and Technology 44: 99-110.

Yu, Q., Niu, F., Pan, X., Bai, Y., and Zhang, M. 2008. Investigation of embankment with temperature-controlled ventilation along the Qinghai-Tibet Railway. Cold Regions Science and Technology 53 : 193-199.

Zarling, J. P., Connor, B., and Georing, D. J. 1984. Air duct systems for roadway stabilization over permafrost areas. Alaska Department of Transportation and Public Facilities. Report No. FHWA-AK-RD-84-10. Juneau, AK 99811.